

RECENT RESULTS ON REACTIONS WITH WEAKLY-BOUND NUCLEI*

M. MAZZOCCO^{a,b}, D. TORRESI^{a,b}, N. FIERRO^a, L. ACOSTA^c
 A. BOIANO^d, C. BOIANO^e, T. GLODARIU^f, A. GUGLIEMMETTI^{e,g}
 M. LA COMMARA^{d,h}, I. MARTEL^c, C. MAZZOCCHI^{e,g}, P. MOLINI^{a,b}
 A. PAKOUⁱ, C. PARASCANDOLO^{a,b}, V.V. PARKER^c, N. PATRONISⁱ
 D. PIERROUTSAKOU^d, M. ROMOLI^d, A.M. SANCHEZ-BENITEZ^c
 M. SANDOLI^{d,h}, C. SIGNORINI^{a,b}, R. SILVESTRI^{d,h}, F. SORAMEL^{a,b}
 E. STILIARIS^j, E. STRANO^{a,b}, L. STROEF^f, K. ZERVAⁱ

^aDipartimento di Fisica e Astronomia, Università di Padova, Padova, Italy

^bINFN — Sezione di Padova, Padova, Italy

^cDepartamento de Física Aplicada, Universidad de Huelva, Huelva, Spain

^dINFN — Sezione di Napoli, Napoli, Italy

^eINFN — Sezione di Milano, Milano, Italy

^fNIPNE, Magurele, Romania

^gUniversità degli Studi di Milano, Milano, Italy

^hDipartimento di Scienze Fisiche, Università di Napoli, Napoli, Italy

ⁱDepartment of Physics and HINP, University of Ioannina, Ioannina, Greece

^jDepartment of Physics, University of Athens, Athens, Greece

(Received January 9, 2013)

Recent results on the reaction dynamics induced by light radioactive ion beams at Coulomb barrier energies are reviewed. As a general feature, the exotic structure and the weak binding energy of most of these projectiles enhance the reaction probability rather than the fusion cross section, as originally expected. The quest has now moved toward understanding which direct reaction mechanism originates the enhancement. Experimental data showed that *n*-halo and *p*-halo nuclei are characterized by a different behavior. Transfer processes enhance the reaction probability for *n*-halo nuclei, such as ^{6,8}He, while for *p*-halo nuclei, such as ⁸B, the breakup channel seems to be mainly responsible for the enhancement.

DOI:10.5506/APhysPolB.44.437

PACS numbers: 25.60.Bx, 25.60.Dz

* Presented at the Zakopane Conference on Nuclear Physics “Extremes of the Nuclear Landscape”, Zakopane, Poland, August 27–September 2, 2012.

1. Introduction

The advent of Radioactive Beam Facilities able to deliver accelerated beams of radioactive isotopes opened the gates to the investigation of the nuclear reactions induced by nuclei far from the valley of β -stability. These nuclei might exhibit exotic features, such as a halo structure, *i.e.* the nucleus can be described as a stable core surrounded by rarefied nuclear matter, or a neutron skin structure, *i.e.* both proton and neutron density distributions can be described by standard parametrizations but with a net excess of neutrons close to the nuclear surface. In addition, as a rather general feature, all these nuclei are very loosely-bound, with proton-, neutron- or alpha-separation energies smaller than 1 MeV. If we just look at the light portion of the nuclide chart, we can find several examples of these peculiar characteristics, for instance the one-proton halo in ${}^8\text{B}$ ($S_p = 137.5$ keV), the one-neutron halo in ${}^{11}\text{Be}$ ($S_n = 504$ keV) and ${}^{15}\text{C}$ ($S_n = 1.218$ MeV), the two-neutron halo in ${}^6\text{He}$ ($S_{2n} = 0.972$ MeV) and ${}^{11}\text{Li}$ ($S_{2n} = 0.300$ MeV) and the neutron skin in ${}^8\text{He}$ ($S_{2n} = 2.140$ MeV).

All these features can influence the reaction dynamics induced by these exotic projectiles and the situation is particularly remarkable at Coulomb barrier energies. In this energy range, in fact, even for reactions induced by stable well-bound projectiles a rather large enhancement of the fusion cross sections was observed. Systematics studies established that either static, such as projectile or target deformations, or dynamical, such as couplings to transfer channels, effects may alter the fusion probability. The development of Radioactive Ion Beams (RIBs) has now led us toward the possibility of performing this kind of studies with exotic projectiles. Unfortunately, these experiments are very demanding in terms of beam intensity, which is still a critical issue for the delivery of secondary beams. For this reason, our knowledge of reactions induced by radioactive projectiles is still limited to nuclei one or two mass unites far from stability. Only very recently ${}^8\text{He}$ - and ${}^{11}\text{Li}$ -induced reactions have started to be investigated.

In this contribution, we will give an overview of the experiments that can be performed with the present-day still limited secondary beam intensity (Sect. 2), then we will present the most relevant achievements obtained so far in this field (Sect. 3) and we will finally concentrate on the our latest experiment to study the system ${}^7\text{Be} + {}^{58}\text{Ni}$ (Sect. 4). Some concluding remarks will be finally given in Sect. 5.

2. Experiments with low-intensity RIBs

RIBs are generally produced with intensities ranging from 10^4 pps (as in the case of ${}^{11}\text{Li}$, ${}^{11}\text{Be}$ and ${}^8\text{B}$)– 10^5 pps (for instance ${}^7\text{Be}$, ${}^8\text{He}$ and ${}^{17}\text{F}$) to 10^7 pps (as for ${}^6\text{He}$). Let us now see what type of nuclear processes we can expect to study with such low beam intensities.

2.1. Elastic scattering

Let us assume we want to study the Rutherford scattering process for the reaction ${}^6\text{He} + {}^{208}\text{Pb}$ at 20 MeV beam energy. How much time do we need in order to accumulate a statistics of 1000 counts in a 3 mm wide \times 50 mm long detector strip at a distance of 70 mm from a 1 mg/cm² thick target?

Table I summarizes the time needed (in hours) to collect 1000 events in strips located at different scattering angles. Due to the strong angular dependence of the Rutherford differential cross section, it is not surprising that the data collection is much faster at the forward than at the backward angles. With a beam intensity of 10⁴ pps, it would take about 39 days to detect 1000 scattering events at $\theta_{\text{lab}} = 90^\circ$, while 21 weeks of beam-time (assuming an unrealistic duty-cycle of 100%) would be needed at $\theta_{\text{lab}} = 150^\circ$. We should remark that all estimates at backward angles are rather optimistic, since they do not take into account the nuclear absorption, whose effects are obviously more relevant at smaller impact parameters.

TABLE I

Time needed (in hours) to collect 1000 Rutherford scattering events in a detector strip 3 mm \times 50 mm located 70 mm far from a 1 mg/cm² thick target. Calculations are performed for the reaction ${}^6\text{He} + {}^{208}\text{Pb}$ at 20 MeV beam energy. Different lines correspond to different beam intensities, while columns refer to detectors strips located at different scattering angles, namely $\theta_{\text{lab}} = 30^\circ$, 90° and 150° .

Intensity (pps)	$\theta_{\text{lab}} = 30^\circ$	$\theta_{\text{lab}} = 90^\circ$	$\theta_{\text{lab}} = 150^\circ$
10 ⁴	18.4	926	3561
10 ⁵	1.84	92.6	356
10 ⁶	0.18	9.3	35.6
10 ⁷	0.02	0.93	3.56

Elastic scattering measurements may sound somewhat “vintage” to the nuclear physics community, but they are sometimes the only experiments that can be performed with limited RIB intensity. These experiments are indeed very meaningful, since the optical model analysis of the elastic scattering differential cross sections provides the total reaction cross section, defined as the sum of the cross sections for all nuclear processes other than the elastic scattering, *i.e.* the cumulative sum of the cross sections for inelastic excitations, transfer channels, breakup processes and fusion. This information tells us about the global “reactivity” of an exotic projectile and this is sometimes the only available piece of information.

2.2. Nuclear processes

Let us now consider whether we might have any chance to measure a nuclear process other than the elastic scattering with low intensity RIBs. Let us suppose we want to investigate a nuclear process (either fusion, breakup or transfer) with an angle-integrated cross section of 1–100 mb. As in the previous case, we will assume the target thickness to be 1 mg/cm² and the detector array geometrical efficiency to be about 10% of 4 π sr. Table II summarizes the time needed (in days) to collect 1000 events over the whole angular range as a function of the secondary beam intensity and of the cross section of the nuclear process.

TABLE II

Time needed (in days) to collect 1000 events over the whole angular range. Calculations are performed assuming a 1 mg/cm² thick target. Different lines correspond to different beam intensities, while columns refer to different cross sections for the nuclear process under evaluation, namely 1 mb, 10 mb and 100 mb.

Intensity (pps)	$\sigma = 1$ mb	$\sigma = 10$ mb	$\sigma = 100$ mb
10 ⁴	4000	400	40
10 ⁵	400	40	4
10 ⁶	40	4	0.4
10 ⁷	4	0.4	0.04

As we can see, the measurement of a nuclear process with a cross section of 1 mb with a secondary beam intensity of 10⁴ pps would require something like 11 years of beam-time (assuming obviously a very efficient 100% duty-cycle!) We can define a process to be “feasibly observable” if we can realistically measure it with an experimental run of about ten days or two weeks, at maximum. For instance, unless we face a process with a very huge cross section, with a secondary beam intensity of 10⁴ pps, such as ⁸B or ¹¹Be, it is nearly impossible to study any reaction mechanism other than the elastic process.

2.3. Hindrance or enhancement?

After we managed to measure the cross section for a relevant nuclear process (*i.e.* fusion, transfer, breakup), we typically aim at determining whether its cross section can be labeled as “standard” or we are facing a hindrance or an enhancement phenomenon. Whenever we speak about hindrance or enhancement it is essential to preliminarily define with respect to what a cross section turns out to be enhanced or hindered. We have two opportunities: to compare our data to theoretical predictions or to other data sets available in literature. In the second case, over the last decade the group of L.F. Canto and P.R.S. Gomes proposed two different approaches.

In the first method [1], they suggested to take into account the different geometrical size of the colliding systems by dividing the cross sections by the factor $(A_p^{1/3} + A_t^{1/3})^2$, being A_p and A_t the projectile and the target mass number, respectively, and to account for the different Coulomb barrier height by multiplying the energy in the center-of-mass system, E_{cm} , by the factor $(A_p^{1/3} + A_t^{1/3})/(Z_p Z_t)$, where Z_p and Z_t are the projectile and target atomic number, respectively. These reductions provide a gross inclusion of the static effects. However, the radial distributions of most of these light exotic projectiles we are interested in, cannot be simply described according to the well-known $A^{1/3}$ -systematics.

To include all static effects, the same group later proposed [2] to use barrier radii, R_B , Coulomb barriers, V_B , and curvatures, $\hbar\omega$, deduced from double-folding potential calculated according to realistic nuclear densities. In this approach, the different system sizes are taken into account by multiplying the cross sections by the factor $2E_{cm}/(\hbar\omega\pi R_B^2)$ and the different Coulomb barrier heights are accounted for by taking the difference $(E_{cm} - V_B)$ and dividing by $\hbar\omega$, *i.e.* the new unit for the energy axis is $(E_{cm} - V_B)/(\hbar\omega)$. Remaining differences between data sets can thus be ascribed to dynamical effects, related to couplings to transfer and breakup channels.

As an example, Scuderi *et al.* [3] showed in a recent publication that the “apparent” enhancement of the subbarrier fusion cross section for the system ${}^6\text{He} + {}^{64}\text{Zn}$ with respect to the reaction ${}^4\text{He} + {}^{64}\text{Zn}$ is clearly understood in terms of the diffuse halo structure of ${}^6\text{He}$. In fact, after applying the normalization prescribed in Ref. [2], the two data sets nearly coincide even in the subbarrier energy regime.

3. Review of recent experiments

We now review some recent results in the investigation of the reaction dynamics induced by light weakly-bound RIBs in the energy range around the Coulomb barrier. We will limit our presentation to a few key systems and, in particular, we will focus on reactions induced on medium-mass (Ni, Cu, Zn) and very heavy (Au, Pb, Bi, U) targets.

3.1. ${}^6\text{He}$ -induced reactions

The first radioactive projectile to be extensively studied from a reaction dynamics point of view was the $2n$ -halo ${}^6\text{He}$ ($S_{2n} = 0.972$ MeV). Early measurements concentrated on subbarrier fusion process. Besides initial claims, it is now well accepted that the halo structure only moderately increases the fusion probability with respect to the corresponding process induced by the stable well-bound counterpart ${}^4\text{He}$ [4–7].

All these studies recorded a fairly large α particle production at near-barrier energies, exhausting about 80% of the reaction cross sections, deduced from elastic scattering experiments. The angular distributions of these particles were peaked around the reaction grazing angles, suggesting direct channels as the main triggering reaction mechanisms. The origin of these α particles was investigated in two series of experiments performed at Notre Dame (USA) and GANIL (France). In the first case, the system ${}^6\text{He} + {}^{209}\text{Bi}$ was studied and it was established that the $2n$ -transfer process was responsible for the 55% of the overall α particle production [8]. The contribution from the $1n$ -transfer process and from the breakup channel was about 20% [9] and 25% [10], respectively. Navin and collaborators studied the system ${}^6\text{He} + {}^{65}\text{Cu}$ and they found that 90% of the α particles were originated by the $2n$ -transfer process and 10% by the $1n$ -transfer channel [11].

3.2. ${}^8\text{He}$ -induced reactions

At GANIL Lemassol *et al.* studied two reactions induced by the weakly-bound neutron skin nucleus ${}^8\text{He}$ ($S_{2n} = 2.140$ MeV): ${}^8\text{He} + {}^{197}\text{Au}$ [12] and ${}^8\text{He} + {}^{65}\text{Cu}$ [13]. The first reaction was investigated in a quite wide energy range between 19.9 and 30 MeV. Very large cross sections for direct reaction processes were measured at subbarrier energies. The good agreement between coupled-channel calculations performed for $1n$ - and $2n$ -transfer channels and experimental data suggests that the breakup channel does not play a crucial role for this system. Concerning the fusion process, only a very moderate enhancement below the Coulomb barrier was observed from the comparisons with the data sets measured for the reactions ${}^{4,6}\text{He} + {}^{197}\text{Au}$.

The experiment aimed at studying the system ${}^8\text{He} + {}^{65}\text{Cu}$ represents perhaps the most challenging experiment performed so far with RIBs, at least in the framework of the reaction dynamics studies. A very complex detector set-up allowed for the simultaneous detection of γ -rays, charged particles and neutrons. The data analysis revealed extra contributions (with respect to statistical model predictions) of the two nuclides ${}^{65,66}\text{Cu}$, which could be explained by the presence of strong $1n$ - and $2n$ -transfer channels, and large yields of γ - ${}^4\text{He}$ and γ - ${}^6\text{He}$ reaction products, also originated from direct reaction mechanisms. The comparison between the reactions ${}^{6,8}\text{He} + {}^{65}\text{Cu}$ showed that the transfer cross sections are larger for the neutron skin nucleus ${}^8\text{He}$ than for the more weakly-bound and halo structure nucleus ${}^6\text{He}$.

More recently the system ${}^8\text{He} + {}^{208}\text{Pb}$ was studied at GANIL and some preliminary results can be found elsewhere in this volume [14].

3.3. The reaction ${}^8\text{B} + {}^{58}\text{Ni}$

The elastic scattering process induced by the $1p$ -halo ${}^8\text{B}$ ($S_p = 137.5$ MeV) on the proton shell closed target ${}^{58}\text{Ni}$ was studied by Aguilera and collaborators at the University of Notre Dame (Indiana, USA) at five energies around the Coulomb barrier [15]. The optical model analysis of the collected data gave a “reduced” total reaction cross section as large as for the $2n$ -halo ${}^6\text{He}$. More recently the same group measured the fusion cross section [16] and more than ten years ago they had measured the breakup process [17] at one colliding energy. As a matter of fact, the sum of the experimental breakup and fusion cross sections exhausts the total reaction cross section. Considering the different fall of the fusion and the reaction cross sections at energies below the Coulomb barrier, there is a rather clear indication that, in this case, the observed enhancement of the reaction probability might be due to the breakup channel instead of transfer channels, differently from what previously observed for the radioactive helium isotopes.

3.4. The reaction ${}^{11}\text{Be} + {}^{64}\text{Zn}$

The scattering process for the interaction of the $1n$ -halo ${}^{11}\text{Be}$ ($S_n = 0.504$ MeV) projectile with a ${}^{64}\text{Zn}$ target was studied by Di Pietro and collaborators [18, 19] at the facility REX-ISOLDE at CERN. A large suppression of the quasi-elastic scattering was observed at small angles and extensive coupled-channel calculations suggest that this outcome may be due to a strong coupling with the breakup channel. The authors observed also a quite large production of ${}^{10}\text{Be}$ ions, whose cross section accounts for half of the reaction cross section. Whether these ${}^{10}\text{Be}$ ions are originated by a projectile breakup process or the $1n$ -transfer channel is still under analysis. Additional details on this experiment can be found in Ref. [19].

3.5. The reaction ${}^{15}\text{C} + {}^{232}\text{Th}$

The fusion–fission cross section induced by the weakly-bound nucleus ${}^{15}\text{C}$ ($S_n = 1.218$ MeV) on a ${}^{232}\text{Th}$ target has been recently studied at ANL (USA) [20]. ${}^{15}\text{C}$ is a quite interesting $1n$ -halo nucleus, which can be described as a ${}^{14}\text{C}$ core coupled to a $s_{1/2}$ loosely-bound neutron. The authors also measured with the same experimental set-up the fusion–fission cross section induced by three lighter carbon isotopes (${}^{12,13,14}\text{C}$) on the same target and in these three cases they found good agreement with coupled-channel calculations, whereas for the system ${}^{15}\text{C} + {}^{232}\text{Th}$ a weak enhancement of a factor 2–5 was observed at the lowest measured secondary beam energies.

4. Preliminary results for the reaction ${}^7\text{Be} + {}^{58}\text{Ni}$

We have recently performed an experiment to investigate the reaction dynamics at Coulomb barrier energies for the system ${}^7\text{Be} + {}^{58}\text{Ni}$. ${}^7\text{Be}$ is a weakly-bound nucleus ($S_\alpha = 1.586$ MeV) with a very well pronounced ${}^3\text{He} + {}^4\text{He}$ cluster structure. The fact that ${}^7\text{Be}$ can break into two stable well-bound charged fragments with similar masses makes this nucleus the most suitable case among all light ions, where the interplay between breakup and transfer processes can be addressed in detail.

The experiment was performed at LNL (Italy), where the ${}^7\text{Be}$ secondary beam was in-flight produced with the facility EXOTIC [21, 22]. We started with a ${}^7\text{Li}$ primary beam delivered by LNL-XTU Tandem accelerator impinging on a H_2 gas target. The primary beam energy and intensity were 34.2 MeV and 100–150 pA, respectively. The target station was kept at an operative pressure of 1 bar and cooled to liquid nitrogen temperature for an equivalent target thickness of 1.35 mg/cm². The ${}^7\text{Be}$ secondary beam was produced via the two-body reaction ${}^1\text{H}({}^7\text{Li}, {}^7\text{Be})n$ with an energy of 23.2 ± 0.4 MeV, a nearly 100-% purity and an intensity about $2\text{--}3 \times 10^5$ pps. A second ${}^7\text{Be}$ energy of 19.0 ± 0.5 MeV was obtained by inserting a 10 μm -thick Al degrader in a suitable location along the beam-line.

Charged reaction products were detected by means of the detector array DINEX [23]. It consisted of four $\Delta E - E_{\text{res}}$ silicon telescopes. The thickness of the inner stages was 40 μm , while the E_{res} were 1000 μm thick. Each detector had an active area of 48.5 mm \times 48.5 mm and both the p -side and n -side were segmented into 16 strips oriented perpendicularly to each other. The telescopes were located at an average distance of 70–72 mm from the 1 mg/cm² ${}^{58}\text{Ni}$ target and covered the polar angle ranges $\theta_{\text{cm}} = 45^\circ\text{--}80^\circ$ and $\theta_{\text{cm}} = 120^\circ\text{--}155^\circ$.

The scattering differential cross section was analyzed in the framework of the optical model by means of the code Fresco [24] to extract the reaction cross section. We obtained a reaction cross section of 480 ± 19 mb for a beam energy of 22.7 MeV at the target middle position. Our result is not in agreement with earlier measurements available in literature in the energy interval 15.1–21.4 MeV [15]. Possible explanations for the origin of the discrepancy may be found in a recent publication [25].

Figure 1 shows a typical $\Delta E - E_{\text{res}}$ matrix collected by the telescope located at forward angles. Continuous lines correspond (from bottom to top) to energy loss predictions [26] for protons, deuterons, tritons, ${}^3\text{He}$, ${}^4\text{He}$, ${}^6\text{Li}$, ${}^7\text{Li}$ ions. Data in Fig. 1 represent only part of the whole statistics collected. We clearly see that the two-dimensional plot is dominated by protons, whose origin is compatible with a fusion–evaporation reaction. As a matter of fact, ${}^4\text{He}$ ions are more abundant than their breakup partners ${}^3\text{He}$. This feature

might indicated that for this reaction the probability for the ${}^3\text{He}$ -transfer is higher than that for the breakup channel. However, a more quantitative analysis of the data is highly necessary before any meaningful conclusion may be drawn.

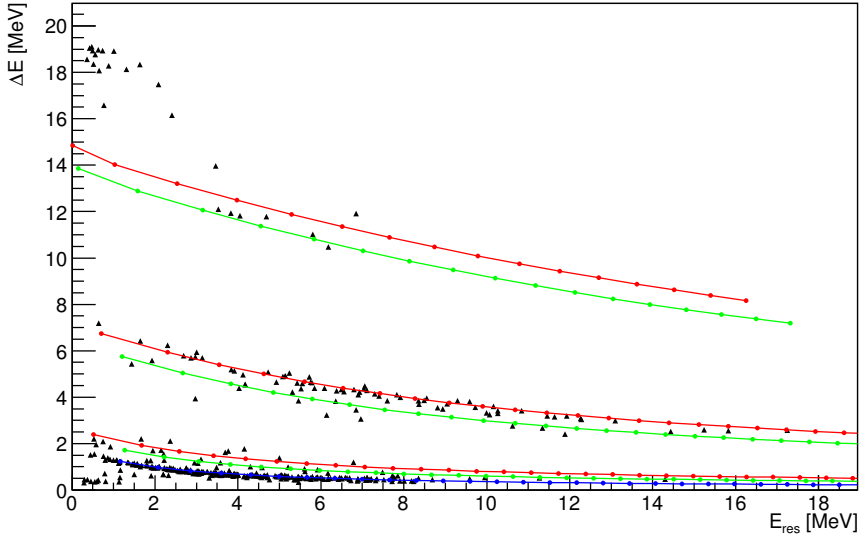


Fig. 1. $\Delta E - E_{\text{res}}$ matrix of charged reaction products detected in the angular range $\theta_{\text{cm}} = 45^\circ - 80^\circ$ for the system ${}^7\text{Be} + {}^{58}\text{Ni}$ at 23.2 MeV beam energy. Lines correspond (from bottom to top) to energy loss predictions [26] for protons, deuterons, tritons, ${}^3\text{He}$, ${}^4\text{He}$, ${}^6\text{Li}$, ${}^7\text{Li}$ ions.

5. Summary

An overview of recent results on the reaction dynamics induced by weakly-bound RIBs at Coulomb barrier energies has been given. The halo structure and weakly-bound nature of these nuclei enhance the reaction cross section rather than the fusion probability. The question has moved toward understanding which direct reaction mechanism triggers this enhancement. Experiments with the $2n$ -halo nucleus ${}^6\text{He}$ and the neutron-skin nucleus ${}^8\text{He}$ indicate the $1n$ - and $2n$ -transfer channels as the main contributors. Experiments with the $1p$ -halo nucleus ${}^8\text{B}$ indicate the breakup channel as the main candidate for the enhancement. Theoretical calculations for the $1n$ -halo nucleus ${}^{11}\text{Be}$ suggest that couplings to breakup channels as mainly responsible for the dumping of the elastic scattering cross section at small angles. Coincidence measurements, as done for the study of ${}^6\text{He}$ and ${}^8\text{He}$, between breakup fragments, though very complicated due to the still low secondary beam intensities, will be needed in the next decade to improve our knowledge of the reaction dynamics at near-barrier energies.

This work was partially supported by the Italian Ministry for Education, University and Research (MIUR) within the project RBFR08P1W2_001 (FIRB 2008).

REFERENCES

- [1] P.R.S. Gomes *et al.*, *Phys. Rev.* **C71**, 017601 (2005).
- [2] L.F. Canto *et al.*, *J. Phys. G* **36**, 015109 (2009).
- [3] V. Scuderi *et al.*, *Phys. Rev.* **C84**, 064604 (2011).
- [4] J.J. Kolata *et al.*, *Phys. Rev.* **C57**, 6 (1998).
- [5] R. Raabe *et al.*, *Nature* **431**, 823 (2004).
- [6] A. Di Pietro *et al.*, *Phys. Rev.* **C69**, 044613 (2004).
- [7] A. Navin *et al.*, *Phys. Rev.* **C70**, 044601 (2004).
- [8] P.A. De Young *et al.*, *Phys. Rev.* **C71**, 051601(R) (2005).
- [9] J.P. Bychowski *et al.*, *Phys. Lett.* **B596**, 26 (2004).
- [10] J.J. Kolata *et al.*, *Phys. Rev.* **C75**, 031302(R) (2007).
- [11] A. Chatterjee *et al.*, *Phys. Rev. Lett.* **101**, 032701 (2008).
- [12] A. Lemasson *et al.*, *Phys. Rev. Lett.* **103**, 232701 (2009).
- [13] A. Lemasson *et al.*, *Phys. Rev.* **C82**, 044617 (2010).
- [14] G. Marquínez-Durán *et al.*, *Acta Phys. Pol. B* **44**, 467 (2013), this issue.
- [15] E.F. Aguilera *et al.*, *Phys. Rev.* **C79**, 021601 (2009).
- [16] E.F. Aguilera *et al.*, *Phys. Rev. Lett.* **107**, 092701 (2011).
- [17] V. Guimaraes *et al.*, *Phys. Rev. Lett.* **84**, 1862 (2000).
- [18] A. Di Pietro *et al.*, *Phys. Rev. Lett.* **105**, 022701 (2010).
- [19] A. Di Pietro *et al.*, *Phys. Rev.* **C85**, 054607 (2012).
- [20] M. Alcorta *et al.*, *Phys. Rev. Lett.* **106**, 172701 (2011).
- [21] F. Farinon *et al.*, *Nucl. Instrum. Methods* **B266**, 4097 (2008).
- [22] M. Mazzocco *et al.*, *Nucl. Instrum. Methods* **B266**, 4665 (2008).
- [23] A.M. Sanchez-Benitez *et al.*, *J. Phys. G* **31**, S1953 (2005).
- [24] I.J. Thompson, *Comput. Phys. Rep.* **2**, 167 (1998).
- [25] M. Mazzocco *et al.*, Proceedings of the International Conference on Nucleus–Nucleus Collisions (submitted).
- [26] J.F. Ziegler *et al.*, *The Stopping and Range of Ions in Solids*, Vol. 1, Pergamon Press, Oxford 1984.